THE ASTROPHYSICAL JOURNAL, 394:288–297, 1992 July 20

THE COOLEST DA WHITE DWARFS DETECTED AT SOFT X-RAY WAVELENGTHS

K. M. KIDDER AND J. B. HOLBERG[1]
Lunar and Planetary Laboratory–West, University of Arizona, 9th Floor, Gould-Simpson Building, Tucson, AZ 85721
M. A. BARSTOW[1] AND R. W. TWEEDY
Physics and Astronomy Department, Leicester University, University Road, Leicester LE1 7RH, England, UK
AND
F. WESEMAEL[1]
Département de Physique, Université de Montréal, CP 6128, Succ. A., Montréal, Québec, Canada H3C 3J7
Received 1991 December 20; accepted 1992 January 29

ABSTRACT

We analyze new soft X-ray/EUV photometric observations of the DA white dwarfs KPD 0631+1043 = WD 0631+107 and PG 1113+413 = WD 1113+413. We also investigate previously reported soft X-ray detections of three other DAs (VR 16 = WD 0425+168, GD 125 = WD 1052+273, and GD 222 = WD 1936+327) and the failure to detect a fourth DA (WD 1910+047) in deep *EXOSAT* observations. New ground-based spectra are presented for all of the objects with *IUE* Lyα spectra for some. This data is used to constrain the effective temperatures and surface gravities. The improved estimates of these parameters are subsequently used to refer a photospheric He abundance for the hotter objects and to elucidate an effective observational low-temperature threshold for the detection of pure hydrogen DA white dwarfs at soft X-ray wavelengths. Last, we present new high S/N spectral data for another DA star (G104−27 = WD 0612+177) which fails to confirm the previous reported detection of He I in that star (Holberg, Kidder, & Wesemael).

Subject headings: stars: abundances — ultraviolet: stars — white dwarfs — X-rays: stars

1. INTRODUCTION

Over 20 hot DA white dwarfs have reported detections at soft X-ray wavelengths, thus far principally with the *Einstein* and *EXOSAT* observatories. These observations, and a handful of others where the hot DA was not detected, have been interpreted in terms of trace helium abundance in the photospheres since helium can provide a strong source of opacity shortward of the He II Lyman limit at 228 Å. Initially, soft X-ray observations were interpreted using chemically homogeneous hydrogen/helium model atmospheres (Kahn et al. 1984; Petre, Shipman, & Canizares 1986; Jordan et al. 1987; Paerels & Heise 1989; Vennes, Shipman, & Petre 1990). An alternative interpretation involving stratified models where a thin layer of H covers the He-rich layer is also possible (Vennes et al. 1988; Koester et al. 1990). The stratified model is the expected equilibrium state of a white dwarf if no forces successfully compete with the gravitational settling of heavier elements. Unfortunately, no definitive observational tests have yet been demonstrated which can distinguish between these two atmospheric configurations.

In and effort to enlarge the data base of DA white dwarf soft X-ray/EUV observations, we have searched the *Einstein* Imaging Proportional Counter (IPC) and the *EXOSAT* Low Energy Imaging Telescopes (LE) observing logs for fields which coincidently contain cataloged DA white dwarfs suspected of being hot enough to be soft X-ray sources. In this paper we discuss three positive detections arising from our search. The results and analysis of the nondetections associated with hot DA white dwarf locations will be reported elsewhere. In addition, we have also reexamined several previously reported soft X-ray observations where the effective temperature of the star was in question. These results are also reported here. In each case the analysis of the broad-band soft X-ray photometry is substantially enhanced by an independent determination of the stars effective temperature and surface gravity. We have used high-quality optical spectra, supplemented with UV spectroscopy for four of the stars, to determine temperature and gravity. We additionally report on the follow-up observations of the reported detection of He I λ4471 in the spectrum of G104−27 (Holberg, Kidder, & Wesemael 1991, hereafter HKW). First, we briefly review the observational status of the six stars in this sample.

KPD 0631+1043 = WD 0631+107.—This white dwarf was first recognized in the Kitt Peak-Downes (KPD) survey of UV-excess objects in the galactic plane (Downes 1986). In spite of its relative brightness ($V = 13.82$) and blue color ($B-V = -0.17$), no follow-up spectroscopic observations appear to have been published. KPD 0631+1043 was independently noted as a serendipitous soft X-ray source in an *Einstein* IPC field by one of us (KK) and by Cordova et al. (1991) as part of independent searches for ultrasoft X-ray sources in the *Einstein* IPC data base.

PG 1113+143 = WD 1113+413.—Detection of this DA has been reported by Giommi et al. (1991) in the *EXOSAT* High Galactic Latitude Survey (HGLS). This same star was noted by us in an earlier IPC image; however, it fell just below our 4 σ detection criterium. Since it was located on the extreme edge of the masked IPC image, we viewed a detection as highly suspect. Unfortunately, it was overlooked in our search of *EXOSAT* images. In view of this detection, we include it among the stars discussed here and analyze both its *EXOSAT*

[1] Guest observer with the *International Ultraviolet Observatory* satellite which is sponsored and operated by NASA, the SERC of the United Kingdom and ESA.

and IPC fluxes. To our knowledge the only previous analysis of this object was by Fleming, Liebert, & Green (1986), who determined $M_v = 10.4$ from the equivalent width of the Hβ line.

VR 16 = WD 0425+168.—As one of the well-known DA white dwarfs in the Hyades cluster, WD 0425+168 has been the subject of numerous observations and studies. Its effective temperature and proximity (~45 pc) indicate that it is a good candidate for detection in the soft X-ray. Stern et al. (1981) provide an upper limit to the *Einstein* IPC flux. Koester et al. (1990) discuss the serendipitous detection of this object in an *EXOSAT* field and determine limits on both the homogeneous and stratified He abundance from the soft X-ray flux. As this object had also turned up in our search, we have independently measured its soft X-ray flux.

GD 125 = WD 1052+273.—Petre, Shipman, & Canizares (1986, hereafter PSC) discuss the marginal detection of GD 125 with the *Einstein* High Resolution Imager (HRI). These authors adopt the conservative view of regarding the observed count rate as an upper limit but point out the low statistical likelihood of a 4 σ background fluctuation in the spatial box containing GD 125. Their case for a possible detection of GD 125 is strengthened by an estimated effective temperature of 26,000 K which they assign this star on the basis of photometry.

GD 222 = WD 1936+327.—PSC quote an upper limit for the *Einstein* HRI flux for this DA. From the lack of detection and their estimated effective temperature of 50,000 K, they determined that the homogeneous photospheric He/H ratio must exceed 10^{-3}.

WD 1910+047.—Margon, Bolte, & Anderson (1987, hereafter MBA), investigating a previously unreported soft X-ray source in *Einstein* IPC images of the SS 433 field, discovered a uncataloged 17th magnitude white dwarf 70″ (1.5 σ) from the location of the soft X-ray source. These authors conducted a thorough spectroscopic and photometric study of this star (WD 1910+047) which showed it to be a DA white dwarf at a distance of ~200 pc and with a modest temperature of 22,000 ± 2000 K. Rejecting alternative hypotheses involving extragalactic and main-sequence coronal sources, they associated the soft X-ray source with photospheric emission from WD 1910+047. In discussing this hypothesis they noted that this object would be among the coolest, if not the coolest, DA yet detected at soft X-ray wavelengths. They went on to point out that the detection of WD 1910+047 implied a relatively large number of similarly cool DA white dwarfs in the temperature range of WD 1910+047 could be expected in soft X-ray/EUV survey missions such as *ROSAT* and *Extreme Ultraviolet Explorer.*

Vennes (1990) further investigated the possibility of photospheric soft X-rays from WD 1910+047. In particular, he modeled the soft X-ray/EUV spectra region and demonstrated that even with a pure hydrogen atmosphere, WD 1910+047 would require an effective temperature of at least 30,000 K, to account for the observed IPC flux. In addition, he compared synthetic spectra to the published Balmer spectra of MBA, finding that an effective temperature as low as 18,000 K could better represent the data. Vennes concluded that if the soft X-ray source of MBA were associated with WD 1910+047, then a photospheric origin for the observed flux could be ruled out.

2. OBSERVATIONS

Lyα profiles for four of our stars were extracted from *IUE* SWP observations. Our treatment of these profiles closely follows that described in Holberg, Wesemael, & Basile (1986, hereafter HWB). However, in a departure from HWB we have applied the temporal corrections for the large- and small-aperture SWP data discussed in Bohlin & Grillmair (1988). In addition, we have also employed the recommended corrections to the SWP wavelength scale (Thompson 1988), where appropriate. Applications of these corrections necessitated a redetermination of the *redwing* correction of the *IUE* absolute sensitivity in the 1150–1350 Å region discussed by HWB. The resulting wavelength-dependent correction of the *IUE* flux scale is quite similar to that found by HWB, but it is now consistent with SWP data corrected to a standard epoch of 1979.9. Such a correction is the short-wavelength analog to the wavelength-dependent sensitivity corrections discussed by Finley, Basri, & Bowyer (1990) for *IUE* data longward of 1320 Å. A full discussion of our SWP sensitivity corrections over the 1150–1350 Å range is given in Kidder (1991). Table 1 lists the UV and optical spectra incorporated in these analyses where the optical data is identified by the appropriate hydrogen Balmer lines.

We obtained high-quality optical spectra of the hydrogen Balmer lines for each of these objects at the Steward Observatory 2.3 m telescope using an 800 × 800 pixel CCD and a 1200 $\mathrm{l/mm^{-1}}$ grating in first order. This configuration provided coverage of the Hδ and Hγ lines at a 2.5–3.0 Å resolution. Due to its faintness, we acquired a higher quality spectrum of the Hγ and Hβ lines for WD 1910+047 at the Multiple Mirror Telescope using a 832 $\mathrm{l\ mm^{-1}}$ grating in second order. The data were reduced using IRAF packages which correct the raw

TABLE 1

UV AND OPTICAL OBSERVATIONS

Object	*IUE* SWP	Aperture Size[a]	t_{exp} (s)	Observer[b]	Balmer Lines
KDP 0631+1043	36005	L	2400	HW	δ, γ, β
	36005	S	1080	HW	...
PG 1113+413	none	...	...	...	δ, γ
VR 16	33108	L	2100	K	δ, γ
GD 125	36006	L	4200	HW	δ, γ
	36008	S	7200	HW	...
	36031	L	2400	HW	...
GD 222	33196	L	720	HW	δ, γ
WD 1910+047	none	...	...	...	γ, β

[a] L, large Aperture; S, small aperture.
[b] K, D. Koester; HW, Holberg & Wesemael.

TABLE 2

SOFT X-RAY OBSERVATIONS

Object	Detector/Filter[a]	Image Number[b]	t_{exp} (s)	Off-axis	Rate (s^{-1})	σ_{rate}
KPD 0631+1043	IPC	5034	2500	25'.4	0.0178	0.0052
PG 1113+413	IPC	488	4900	29.4	0.0074	0.0045
	3Lx	85.330	26611	25.6	0.0098	0.002
	3Lx	85.335	20081	26.9	0.014	0.002
VR 16	4Lx	84.280	12633	20.9	0.013	0.002
WD 1910+047	3Lx	84.108	18505	12.6	<0.0053	...
	3Lx	84.269	18795	13.0	<0.0034	...
	3Lx	85.137	16199	13.3	<0.0048	...
	Al/P	85.138	22115	13.3	<0.0054	...

[a] *EXOSAT* LE1 filters: 3Lx, thin lexan; 4Lx, thick lexan; Al/P, aluminum/paralyene.
[b] Year.day of year for *EXOSAT* observations and sequence number for *Einstein* images.

images for electronic biases, dark current, pixel-to-pixel variations and image distortion. The sky-subtracted columns were summed into a single spectrum, then they were assigned fluxes using the observations of several well-known DA white dwarf standard stars. The authors would like to note that the spectra presented here represent only a fraction of the data from a much more extensive list of known hot DA white dwarfs which includes most of the currently known soft X-ray sources. Results of these observations are reported in Kidder (1991).

The *Einstein* IPC and *EXOSAT* LE data bases were searched at positions of cataloged DA white dwarfs for possible serendipitous occurrences. As a result, a new source was noted in an IPC image, a marginal detection of another source in another IPC image, and a third source in a thin lexan filter image of the *EXOSAT* LE1 telescope. These sources coincide with the locations of KPD 0631+1043, PG 1113+413, and VR 16, respectively. We also examined several long exposure *EXOSAT* fields containing WD 1910+047 from which no source was observed, so upper limits to the count rate were determined. The image numbers, total on-target exposure times, and the angular separation between the white dwarf and the image center are listed in Table 2 along with derived corrected soft X-ray count rate or the 3 σ upper limit. The raw soft X-ray count rates were extracted from the IPC and *EXOSAT* images in a similar procedure. Spectral information could not be derived from the IPC images, so the softest energy channels (1–5) were added together. Also, the source and background counts were measured with rather large box sizes ($\sim 6' \times 6'$) in an effort to minimize the uncertainties resulting from the broadening of the point spread function for soft photons incident at large field angles. The net background subtracted counting rates were also corrected for vignetting at the position of the source in the field. The *EXOSAT* images, on the other hand, were measured with the standard processing software at the University of Leicester using a source box size of $100'' \times 100''$ (see Barstow & Tweedy 1990). These count rates were then corrected for the predicted fraction of source count rate uncertainties and the 3 σ upper limits listed in Table 2.

3. DETERMINATION OF TEMPERATURE AND GRAVITY

Detailed synthetic hydrogen line profiles are a powerful means of determining a DA white dwarf's atmospheric temperature and gravity. For the analysis of the optical/UV spectra, we exclusively employ pure hydrogen, plane parallel geometry, LTE white dwarf model atmospheres which include hydrogen line-blanketing for Lα-Lδ and Hβ-Hϵ using the detailed line broadening theory of Vidal, Cooper, & Smith (1973). These models are essentially extensions of Wesemael et al. (1980) computed with detailed flux points in the mentioned line profiles. This grid of more than 100 independently generated models consists of 33 temperatures ranging from 16,000–70,000 K for surface gravities of log $g = 7.5$, 8.0, and 8.5. Additional models at $T_{eff} = 13{,}000$ and 14,000 K for log $g = 8.0$ and a set with $T_{eff} = 40{,}000$–70,000 K for log $g = 7.0$ are also incorporated. The computed emergent fluxes can be related to the observed visual magnitude (V) at 5500 Å through the relation

$$f_v = 3.57 \times 10^{-20} \times 10^{-0.4xV}(\mathrm{ergs\ s^{-1}\ cm^{-2}\ Hz^{-1}}) \quad (3.1)$$

based on the absolute calibration of Vega by Tüg et al. (1979).

Our procedure for determining the effective temperature and surface gravity of a hot DA white dwarf is similar to that described in HWB and Kidder (1991) where chi-squares (χ^2) are computed between the observed line profile and an effective temperature versus surface gravity grid of synthetic line profiles. Our χ^2 grids are composed of 51×41 points where each point (T_{eff}, log g) reflects the parameters of a synthetic spectrum interpolated from the model grid. The best-fitting parameters are determined from the minimum χ^2 of the combined grids of the available line profiles, and the uncertainties in these parameters are estimated from the variance of the fits for the individual line profiles. The 1 σ and 3 σ confidence regions for the temperature and gravity determined from each profile are shown in the plots of Figure 1. Independently analyzing each line profile in this way provides a strong test of both the mutual consistency of the data set and the completeness of the models over a range of wavelengths. The adopted atmospheric parameters are listed in Table 3, and comparison plots of the model spectra to the observed spectra are shown in Figure 2 and Figure 3. The V magnitudes in Table represent averages obtained from various published photometry listed in McCook & Sion (1987), and in particular from Kidder, Holberg, & Mason (1991), which includes *UBV* photometry for five of these stars.

Each line profile is defined for fitting purposes to encompass nearly the entire equivalent width without overlapping an adjacent profile. The synthetic Balmer profiles are individually converted to a residual intensity scale by selecting continuum levels in the far wings of each line. The observed spectra are converted in the same way before the χ^2 is computed. This procedure helps to reduce the sensitivity of our results to errors in fluxing and to make them somewhat independent of the local slope of the continuum. The synthetic Lyα fluxes, on the other hand, are normalized to the adopted visual magnitude (see Table 3) taking advantage of the spectrophotometric cali-

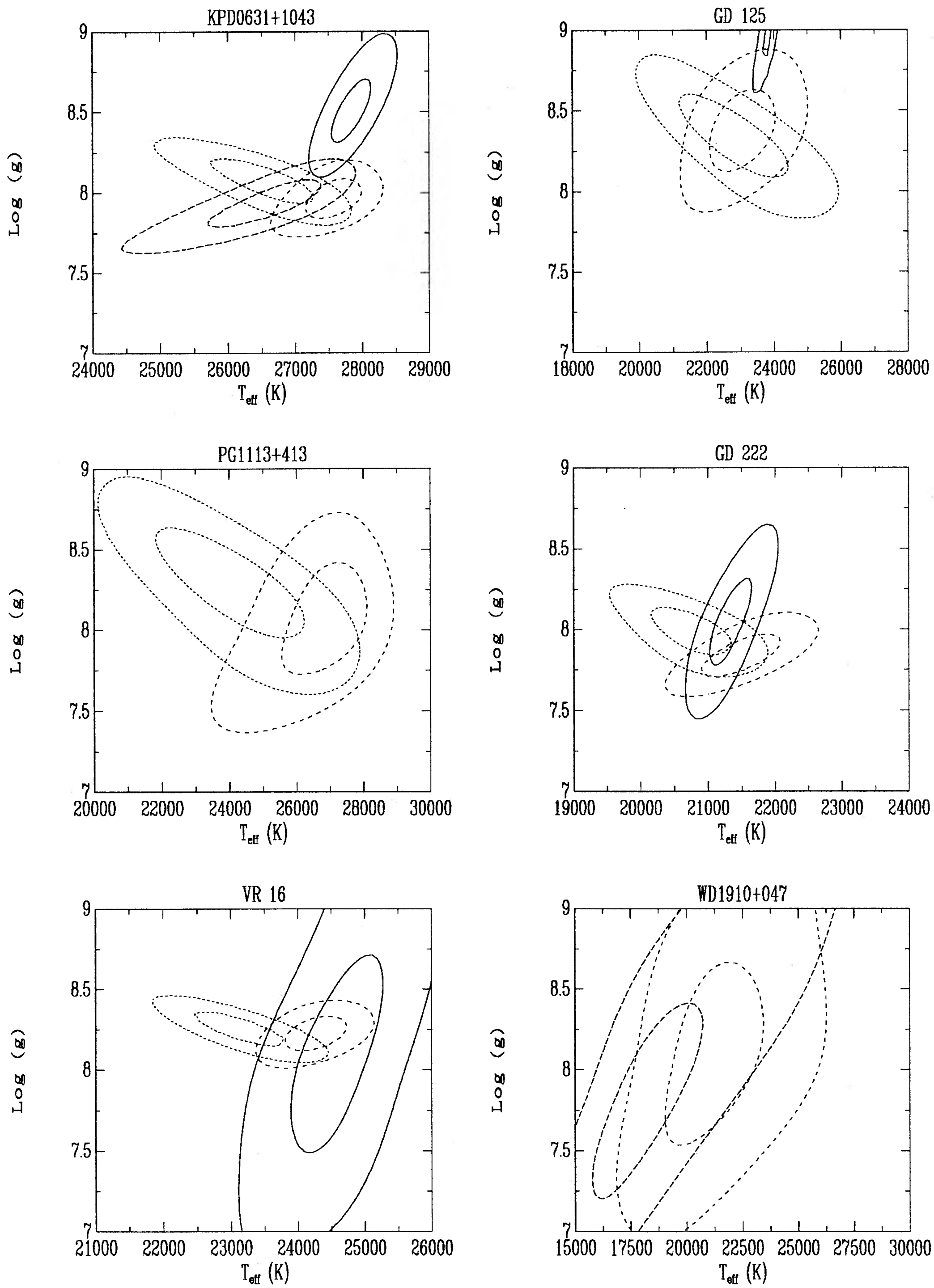

FIG. 1.—Contours of equal χ^2 for each of the stars in this sample. Each set of two contours enclose the 1 σ and 3 σ joint confidence regions for the line profiles of Lα (*solid lines*), Hβ (*longest dashes*), Hγ (*middle dashes*), Hδ (*shortest dashes*).

bration of *IUE*. The effective leverage obtained from normalizing the UV spectra in the optical increases the sensitivity of the results to the slope of the continuum, therefore, the effective temperature. In addition, the synthetic spectra are convolved with a kernel characteristic of the instrumental spectra resolution. The FWHM of the Gaussian kernels applied to the *IUE* and ground-based data are 5.75 and 3.0 Å, respectively.

4. ANALYSIS OF SOFT X-RAY FLUXES

4.1. *Modeling Considerations*

For the soft X-ray analysis we are able to compare results using two different grids of model atmospheres. The first is essentially the soft X-ray/EUV extension of the models from F. Wesemael, which we used in the optical/UV analysis. In the

TABLE 3

SUMMARY OF ADOPTED ATMOSPHERIC PARAMETERS

Object	V	σ_V	T_{eff}	$\sigma_{T_{eff}}$	log g	$\sigma_{\log g}$	log He/H
KPD 0631+1043	13.82	0.01	27200	400	8.00	0.13	< -4.2
PG 1113+413	15.38	0.05	26200	1100	8.05	0.15	< -5
VR 16	14.03	0.01	24000	500	8.15	0.18	< -5
GD 125	14.12	0.02	23400	500	8.50	0.19	Indefinite
GD 222	13.59	0.01	21200	300	7.85	0.13	Indefinite
WD 1910+047	16.91	0.01	20100	1500	8.10	0.25	Indefinite

short-wavelength region the grid includes models for T_{eff} = 20,000(2000)30,000 K and log g = 7.0(0.5)8.5. The second grid of models was computed using an LTE code as described in Barstow (1990) for hydrogen-rich compositions, 10^8 cgs gravity with several uniform abundances of trace helium. This grid consists of the emergent fluxes from the soft X-ray to the near IR for photospheric temperatures from 20,000 to 200,000 K and homogeneous helium abundances of log He/H = -1, -2, -3, -4, -5, $-\infty$. Note that line blanketing is *not* included in these model computations.

The soft X-ray flux from DA white dwarfs is a strong function of the effective temperature and considerably less dependent on the surface gravity, which for most of the cases considered here are near log g = 8.0. This value will be assumed for the subsequent analysis of He abundance. Also, on a practical level there should be no inconsistency introduced by using pure hydrogen models for the determination of temperature and gravity and using hydrogen/helium models to determine He abundance. At the trace He abundances we are concerned with here, helium has no discernible impact on the optical or UV spectra of these stars. On the other hand, line-blanketing in model atmosphere codes is important to the soft X-ray/EUV fluxes in the temperature range of 20,000–30,000 K. In effect the difference in the photometric count rates obtained from the two sets of models behaves like a shift in temperature. We use the unblanketed models in this analysis only when necessary to determine a nonzero helium abundance then with consideration of the effect of line blanketing to the fluxes within the instrumental bandpass.

The theoretical instrumental count rate which we can compare to the observed count rates of Table 2 are computed as follows:

$$n(\mathrm{s}^{-1}) = 4\pi \frac{R^2}{D^2} \int_0^\infty H_\nu A_\nu e^{-\tau_\nu} d\nu , \tag{3.2}$$

where R^2/D^2 is the solid angle computed from the V magni-

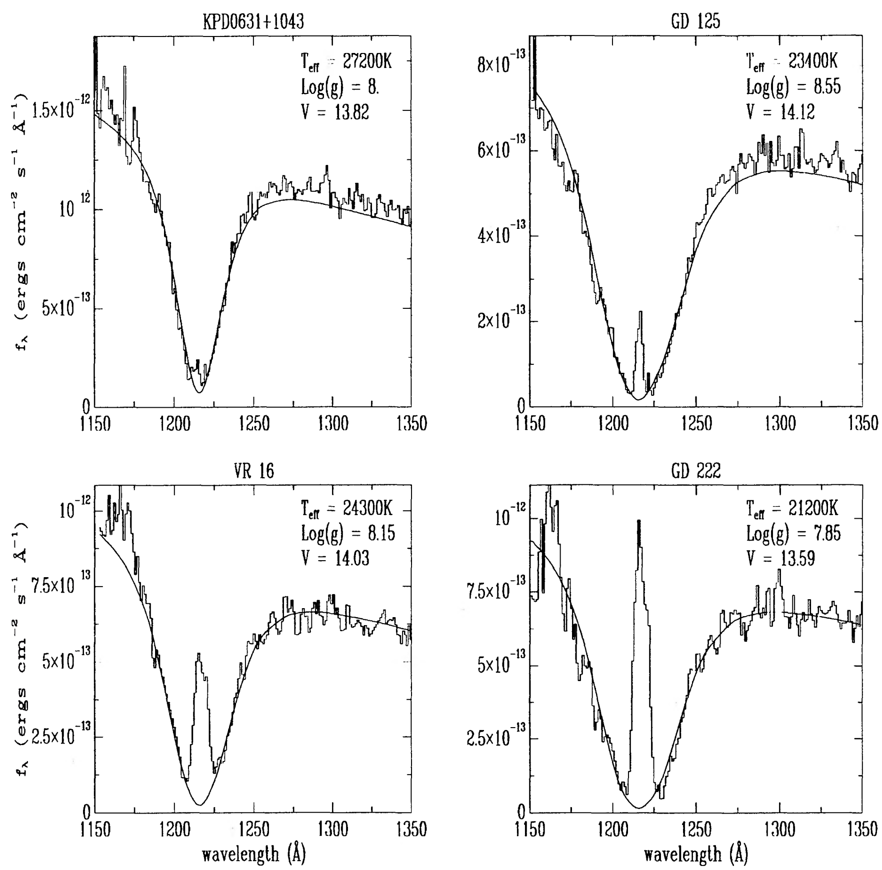

FIG. 2.—Best-fit synthetic spectra (see Table 3) compared with the observed Lyα profiles

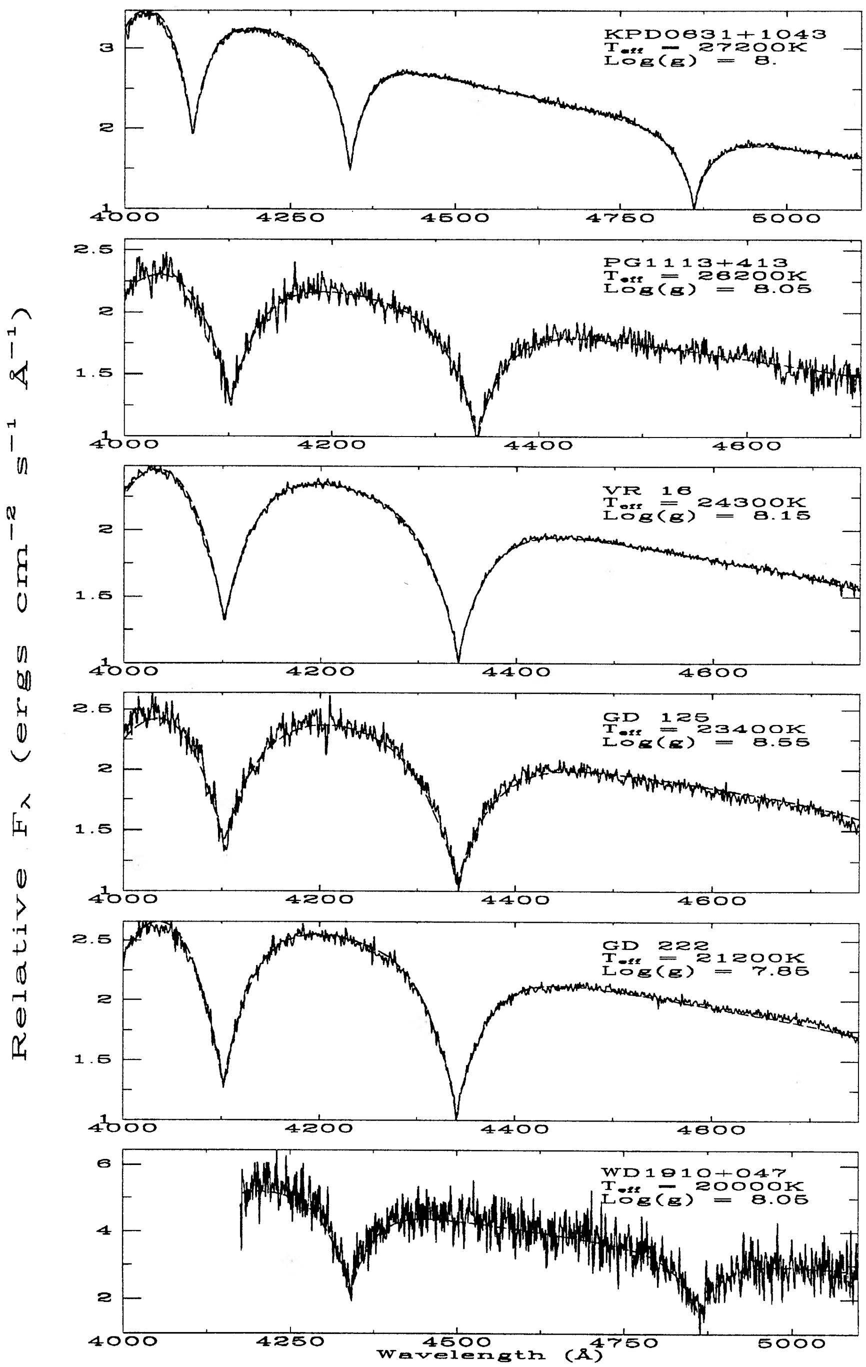

FIG. 3.—Best-fit synthetic spectra (see Table 3) compared with the observed Balmer line profiles. The synthetic spectra have been scaled to minimize the χ^2.

tude using equation (3.1) and $f_\nu = 4\pi R^2/D^2 H_\nu$. H_ν is the predicted emergent synthetic stellar flux, A_ν is the instrumental effective area for the location of the object in the field, and τ_ν, represents the optical depth of the interstellar medium along the line of sight. The instrumental effective area for the observation is interpolated from the integrated telescope on-axis response function and its relative sensitivity across the field view. The interstellar optical depth is computed from the product of the photoelectric cross sections of Morrison & McCammon (1983) and the interstellar column density of neutral hydrogen ($N_{\rm H}$).

4.2. *Helium Abundance Interpretation*

In this section we compare the observed soft X-ray/EUV count rates listed in Table 2 with theoretical instrumental count rates in an effort to determine limits to the photospheric He abundance for KPD 0631+1043, PG 1113+413, and VR 16. Two grids of synthetic count rates as a function of $T_{\rm eff}$ versus log He/H, one for $N_{\rm H} = 10^{18}$ and the other for $N_{\rm H} = 10^{19}$ cm^{-2}, were computed for the hottest star in our sample KPD 0613+1043. Plotted along with the observed count rates contours in Figure 4 are the 1 σ temperature constraints deter-

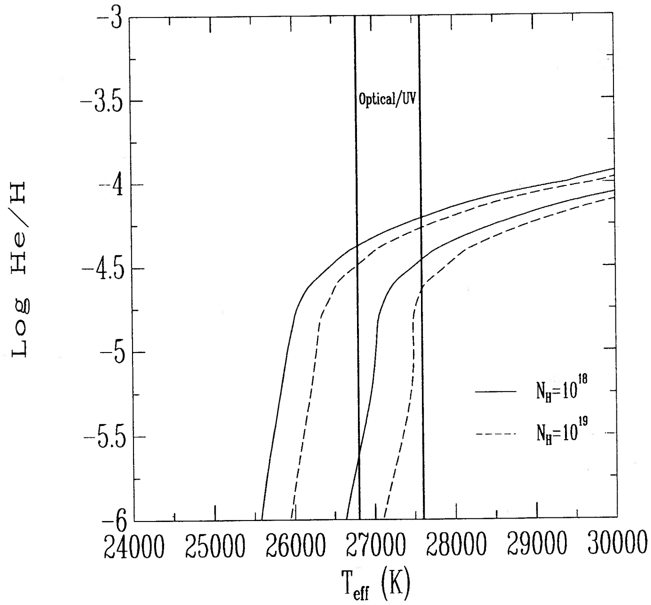

FIG. 4.—Contours (1 σ likelihood) for the observed soft X-ray count rates for KPD 0631+1043 plotted along with its spectroscopically determined temperature range (1 σ). The limited effect of the ISM is shown with contours for H column densities of 10^{18} (*solid curves*) and 10^{19} cm^{-2} (*dashed lines*).

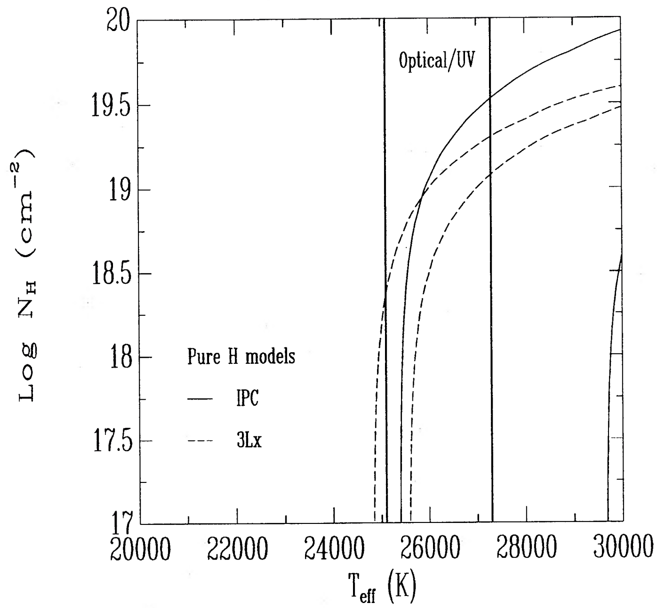

FIG. 5.—Contours (1 σ likelihood) for the observed soft X-ray count rate of PG 1113+413 as observed with the *Einstein* IPC (*solid lines*) and the thin lexan filter (*dashed lines*) of *EXOSAT*. The models assume a pure H atmosphere with an interstellar H column of 10^{19} cm^{-2}.

mined from the optical/UV analysis. The above range expected for the interstellar hydrogen column is estimated from H I maps of the local ISM (Paresce 1984) in the direction of KPD 0631+1043 ($l = 201°.4$, $b = 1°.0$) at its expected distance of ~ 50 pc which we obtain from the adopted parameters and the Hamada-Salpeter zero-temperature radius (Hamada & Salpeter 1961). Since most of the interstellar absorption occurs at longer wavelengths than the IPC bandpass, the solution for the He abundance is essentially insensitive to the interstellar column over this range. From a comparison of the blanketed and unblanketed models for a pure hydrogen atmosphere, the effect of hydrogen line blanketing on the fluxes in the IPC bandpass can be interpreted as an apparent shift of the contours of +750 K which would in this case allow a pure hydrogen solution at the cooler end of the temperature range. Therefore, we deduce an upper limit of He/H $< 10^{-4.2}$ for the homogenous He abundance.

The contours for the IPC and the thin lexan filter count rates are plotted for PG 1113+413 in Figure 5; this time as a function of T_{eff} verses N_H. Since PG 1113+413 is slightly cooler and fainter than KPC 0631+1043, detection of this star in the IPC implies that its photosphere is virtually pure hydrogen. This observation is reinforced by the *EXOSAT* data. Two-color photometry for hotter stars usually provides a unique solution for the He abundance and the interstellar column, but the results in this case are limited by the uncertainty of the weak IPC flux. Estimating the distance to PG 1113+413 from its adopted parameters locates it at a distance of ~ 100 pc. Since we are not aware of an independent determination of the interstellar column near PG 1113+413 ($l = 171°$, $b = 66°$), we instead use the mean local interstellar density of 0.07 cm^{-3} (Paresce 1984) to estimate $N_H \sim 2 \times 10^{19}$ cm^{-2}. In view of its high galactic latitude, we regard this column more as an upper limit. This and the temperature range deduced from the line profiles reinforce the conclusion that PG 1113+413 has a virtually pure hydrogen atmosphere (He/H $< 10^{-5}$).

Last, VR 16 has one of the lowest effective temperatures ($T_{eff} = 24{,}000 \pm 500$ K) of any DA detected at soft X-ray wavelengths. Its observation at soft X-ray wavelengths is also a clear indication that its photosphere is virtually pure hydrogen (He/H $< 10^{-5}$), otherwise detection of this star would *not* have been possible. As in the case of PG 1113+413, a grid of synthetic count rates was computed as a function of T_{eff} versus N_H using the pure hydrogen line-blanketed model atmospheres. Figure 6 indicates that within the 1 σ constraints, a pure hydrogen model mutually satisfies both the soft X-ray and the optical/UV constraints when the interstellar column is less than 7×10^{19} cm^{-2}. The second set of soft X-ray count rate contours in Figure 6 are shown to illustrate the effect line blanketing has on the models fluxes through the thick lexan filter bandpass.

4.3. *Detection Threshold for the Coolest Hot DAs*

It is widely expected from the successful operation of the *ROSAT* and the soon to be launched EUVE missions that hot DA white dwarfs will constitute a significant fraction of sources observed at soft X-ray wavelengths (Finley, Malina, & Bowyer 1987; Barstow 1989). Both of these missions involve all sky surveys at EUV wavelengths longward of 100 Å; therefore, the number of DA white dwarfs available for study at these wavelengths is expected to increase dramatically. Since the soft X-ray flux is a strong function of temperature, the issue of the effective temperature which nearby pure hydrogen DA white dwarfs begin to be readily detected is of some importance.

Shown in Figure 7 are the contours for the on-axis theoretical count rates of a pure hydrogen DA white dwarf as observed through three different soft X-ray/EUV bandpasses (*Einstein* IPC, thin lexan and aluminum/paralyene of the *EXOSAT* LE1). The models assume a pure hydrogen atmosphere and an interstellar column density of 10^{18} cm^{-2}. Two contours of predicted count rates are displayed for each instrument as a function of effective temperature and visual magnitude

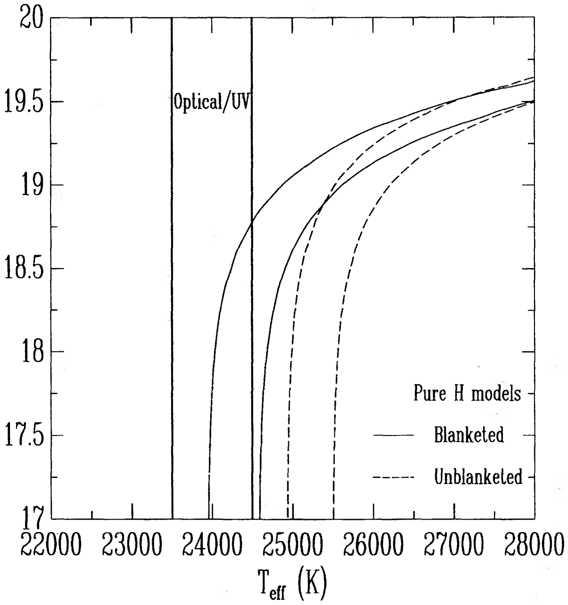

FIG. 6.—Contours (1 σ likelihood) for the observed soft X-ray count rate of VR 16 for a pure H atmosphere along with its spectroscopically determined temperature range (1 σ). Also shown for comparison is the difference in count rate obtained by incorporating line blanketing into the model atmosphere calculations.

(observers coordinates). The leftmost set of contours correspond to a count rate of 0.005 s^{-1} which is a typical detection threshold for white dwarfs and the second set for a firm detection count rate of 0.05 s^{-1}. The thin lexan appears as the most sensitive instrument of these three to the soft X-ray spectrum of moderately hot DAs. In addition, the *Einstein* HRI, not shown, is intrinsically less sensitive to the softest sources.

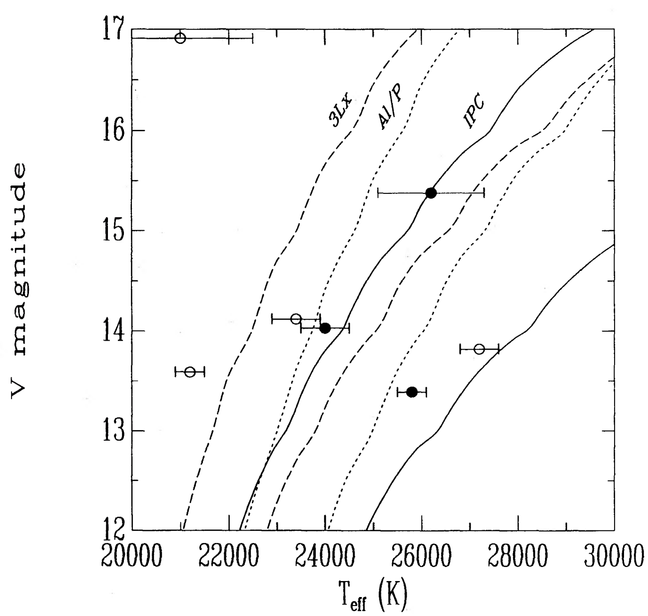

FIG. 7.—Contours of theoretical instrumental count rate of 0.005 and 0.05 s^{-1} as observed with the *Einstein* IPC (*solid lines*) and the thin lexan filter (*dashed lines*) and the aluminum/paralyene filter (*dotted lines*) of the *EXOSAT* LE1. All models assume a pure hydrogen, line-blanketed, 10^8 cgs gravity atmosphere with the interstellar absorption of a H I column of 10^{18} cm^{-2}. The plotted data points correspond to the effective temperatures and apparent visual magnitudes of the stars discussed in this paper. Soft X-ray detections are distinguished from nondetections by filled and open circles, respectively.

The adopted parameters of KPD 0631+1043, PG 1113+413, VR 16, GD 125, GD 222, and WD 1910+047 are also plotted in Figure 7. This representation illustrates the relative sensitivity of the *Einstein* and *EXOSAT* instruments to moderately hot DA white dwarfs as a function of temperature and the apparent visual magnitude. The three hotter sources which were detected obviously lie above the threshold for detection. However, using our estimate of effective temperature of GD 125 (23,400 K), this DA appears to be cool enough to call into question the detection of photospheric soft X-rays with the *Einstein* HRI. Furthermore, we can conclude that GD 222 and WD 1910−047 with temperatures of 21,200 and 20,100 K, respectively, are even less likely to have detectable photospheric emission at soft X-ray wavelengths. As can be seen in Figure 7, pure H white dwarfs cooler than ~23,000 K are unlikely to be detected at soft X-ray wavelengths.

5. DISCUSSION

Our adopted effective temperatures and surface gravities, as determined from optical/UV spectroscopy, and the adopted V magnitudes with their associated uncertainties are given in Table 3. We also list the corresponding homogeneous He abundances which were determined from the soft X-ray/EUV data. In the cases where the DA is found to be too cool and faint to have been reliably detected at soft X-ray wavelengths we have assigned an "indefinite" He abundance value. Next, we summarize and discuss each of cases.

KPD 0631+1043.—No prior analysis of either the optical/UV spectra of this star or its soft X-ray flux exist. Our analysis of the Balmer profiles (β, γ, and δ) yields the best-fitting parameters of $T_{eff} = 27{,}200$ K and $\log g = 8.0$. The Lyα profile, on the other hand, is best fit by $T_{eff} = 28{,}000$ K and $\log g = 8.5$. Better agreement between these two results can be achieved if the observed visual magnitude of KPD 0631+1043 was increased slightly by ~0.05 mag. However, on the basis of the results of the UBV photometry of Kidder, Holberg, & Mason (1991) an adjustment of this size does not appear to be possible. Other possible effects which could influence the UV, as interstellar reddening of contamination of the V band by a faint companion would increase the observed discrepancy. We adopt here a best fitting model in which both the T_{eff} and $\log g$ are defined by the optical data but the uncertainties are large enough to be compatible with the Lyα.

PG 1113+413.—This is the first analysis which we are aware of the soft X-ray detection of this DA. Using the results of the Balmer line profile fits, ($T_{eff} = 26{,}200 \pm 1100$ K and $\log g = 8.05 \pm 0.15$) and the observed IPC and *EXOSAT* count rates, we conclude that PG 1113+413 must have a photospheric He abundance of He/H < 10^{-5}.

VR 16.—As mentioned previously, Koester et al. (1990) discuss the *EXOSAT* observations of VR 16. Based on Balmer equivalent widths, they obtained $T_{eff} = 26{,}000 \pm 2000$ K for a $\log g = 8.0$ DA white dwarf. Our results are in essential agreement with theirs; however, our joint analysis of the hydrogen line profiles sufficiently restricts the temperature of this DA such that it can now be seen to lie near the low end of temperatures considered by Koester et al. (1990). Our Lyα and Balmer results yield a consistent $T_{eff} = 24{,}300 \pm 840$ K and $\log g = 8.15 \pm 0.10$. In light of this, VR 16 must have a nearly pure hydrogen photosphere which we assign a homogeneous number ratio of He/H < 10^{-5}. Alternatively, the helium abundance can be expressed as a hydrogen layer mass $M_{\rm H} > 3.3 \times 10^{-14} M_\odot$, which is derived from the tables in Koester et al. (1990). It is interesting to note here that VR 16 most nearly resembles CoD $-38°10980$ in terms of its atmospheric parameters. Together these two stars represent the coolest DAs which have been convincingly detected at soft X-ray wavelengths.

GD 125.—We presented an analysis of the *IUE* and ground-based spectroscopy and broad-band photometry which indicated that a more reliable estimate for the temperature of GD 125 is 23,400 K; cool enough to call into question the HRI detection of photospheric soft X-rays from this star. PSC using published photometry estimated a temperature of 26,000 K. On the basis of this and the observed HRI count rate they estimated a He abundance of He/H = 1–5 $\times 10^{-5}$. While there is some difference between gravities found from the *IUE* and ground-based results, which can be reconciled if the observed *V* magnitude were brightened by 0.03, the temperature estimate of 23,400 K still remains consistent between the two sets of data. GD 125 thus presents an interesting case. If the HRI detection of PSC is accepted, then GD 125 would be the coolest DA soft X-ray source. On the other hand from the discussion of DA detectability verses effective temperature for the softer, more sensitive *EXOSAT* data leads one to predict that GD 125, even with a pure H atmosphere, should not have been detected with the HRI. Therefore, a He abundance could not be determined for this star.

GD 222.—Our Balmer and Lyα spectra yield a very consistent result of $T_{\rm eff} = 21{,}200 \pm 380$ K and $\log g = 7.85 \pm 0.17$ for this star. This result is also consistent with the photometric results of Gusienov, Novruzova, & Rustamov (1983). A somewhat higher $T_{\rm eff} = 23{,}265 \pm 143$ K is obtained by McMahan (1989). None of these results, or any other that we are aware of, is remotely close to the 50,000 K estimate used by PSC. H. L. Shipman (private communication) informs us that the temperatures in PSC were obtained on the basis of the data available at the time which for this object consisted of Johnson *UBV* colors. He feels that a temperature determination from the Lyα profile clearly supersedes the earlier work and while the discrepancy is surprisingly large, he believes that the lower temperature is probably correct. We conclude that GD 222 with a temperature of 21,200 K is too cool to be a soft X-ray source, therefore, the He abundance cannot be determined from this data.

WD 1910+047.—We have further investigated WD 1910+047 by searching several deep *EXOSAT* fields containing WD 1910+047 and employing new optical spectra of this DA. The results, summarized in Table 2, show no X-ray source present at the location of WD 1910+047. Taken individually or together our observed *EXOSAT* count rates correspond to an upper limit on the soft X-ray flux from WD 1910+047, 5–10 times *lower* than the IPC flux detected by MBA.

Vennes (1990) in his examination of the question of photospheric soft X-ray emission from WD 1910+047 showed that the published optical spectra of MBA was consistent with an effective temperature as low as 18,000 K. The analysis of our Balmer profile data yield an effective temperature of $T_{\rm eff} = 20{,}000 \pm 380$ K intermediate between that of MBA and Vennes, yet this is still far too cool to produce the observed IPC flux. This confirms the primary conclusion of Vennes that WD 1910+047 is too cool to be the source of soft X-rays. We have also examined the regions of the *EXOSAT* fields which correspond to the celestial coordinates of the source as determined by MBA from the IPC images. We find no obvious source at this location in any of the *EXOSAT* images listed in Table 2.

We conclude, along with Vennes (1990), that WD 1910+047 is too cool to be the source detected by MBA. Moreover, this source evidently is not present during the 1984–1985 epoch of the *EXOSAT* observations, at the position determined by MBA for the centroid of the IPC source. The source reported by MBA is likely transient in nature and ultimately unrelated to WD 1910+047.

G104−27 = WD 0612+177.—HKW reported the detection of a weak feature due to He I λ4471 in three high signal-to-noise spectra of G014−27, a 26,000 K DA. From the observed strength of these features, HKW obtained estimates of a homogeneous He/H ratio of $\log {\rm He/H} = -2.56 \pm 0.26$ or alternatively a stratified H envelope mass of $\log M/M_\odot \sim 16.6 \pm 0.3$. Such estimates are consistent with He soft X-ray opacity being responsible for the failure to detect this star with *EXOSAT* (Paerels & Heise 1989).

We present here follow up optical observations of G104−27 in which the 4471 Å feature is not evident at the strength of the earlier observations. In Figure 8 we show 10 individual spectra of G104−27 obtained over a 2 yr period; including the original spectra of HKW. The follow up spectra shown in Figure 8 were obtained with the same instrumentation and have similar or better signal to noise, to the original observations of 1989 February. Conservative upper limits to possible features at 4471 Å in these later spectra are all 75 mÅ or lower. This is in contrast to the measured equivalent widths of 366 $\pm$ 40 mÅ and 319 $\pm$ 30 mÅ and 204 $\pm$ 30 mÅ observed in the three 1989 February spectra. In light of this apparent discrepancy we have reexamined the original observations of HKW with respect to any observational or data analysis procedures which might be responsible for possible spectral artifacts corresponding to the 4471 Å features. This reexamination included an independent

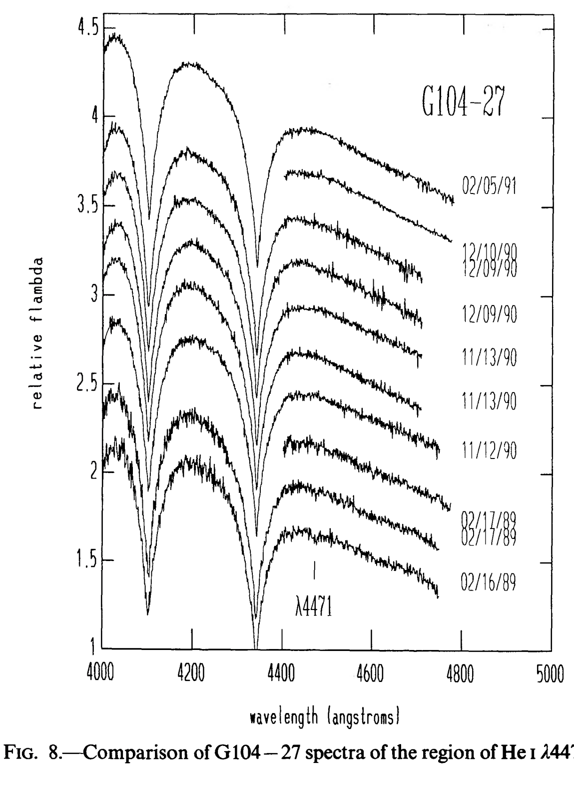

FIG. 8.—Comparison of G104−27 spectra of the region of He I λ4471

reduction of the original data sets. We were unable to find a procedure or effect which would produce such an artifact. As mentioned in HKW, no spectra or other DA stars observed on those two nights yielded similar features, in addition, one of the three spectra was intentionally obtained at a separate grating setting to confirm the presence of the feature which was evidently in the raw spectra obtained at the telescope.

If the original observations are accepted as valid, then the failure to detect the He I $\lambda 4471$ feature 21 months later presents a dilemma. We offer here two possible interpretations for the case of G104−27 which might account for the temporal variations of the strength of He I features. One interpretation is that photospheric He may not be distributed uniformly over the surface of G104−27; possibly due to the presence of a magnetic field and a slow stellar rotation which leads to a modulation of He I line strengths. This is the model favored to explain the spectral variations in the well-known magnetic white dwarf Feige 7 (Achilleos et al. 1992). This scenario would have certain similarities to the model of V471 Tauri, in which Barstow et al. (1991) describe the observed modulation of soft X-ray/EUV flux as a rotation effect produced by enhanced soft X-ray/EUV opacity in the polar regions of the DA white dwarf component of the V471 system. The polar opacity, in this instance, is due to magnetically confined accretion of He and metal-rich material from the wind of the K companion. In G104−27 there is no binary accretion, however, He-rich patches coupled with slow rotation could lead to a modulation of the strength of He I feature. Since many white dwarfs are known to be slow rotators (Pilachowski & Milkey 1984) and some exhibit virtually no rotation at all (Schmidt 1987) such long-term rotational modulation would not be entirely without support.

A second possible interpretation is much more interesting from the stand point of the evolution of white dwarf photospheres. In a comprehensive model of white dwarf spectral evolution proposed by Fontaine & Wesemael (1987), the dramatic changes observed in the non-DA to DA population ratio as a function of effective temperature is a consequence of the development of thin H photospheres due to gradual accumulation of surface H from the outward diffusion residual H in the mantle of white dwarfs. By the time a star has reached $\sim 45{,}000$ K the process of H accumulation has progressed to the point that all white dwarfs are DA in appearance and no DB white dwarfs are observed in the range 45,000–30,000 K, the "DB Gap." At the red edge of the DB Gap the onset of near surface convection can mix He into the photospheres of those stars having the thinnest H layers and DB stars can appear. As noted in HKW, G104−27 lies tantalizingly near the red edge of the DB gap. It is not inconceivable that we are witnessing the onset of a change in the spectral character of G104−27 related to convection included mixing of subphotospheric He into the photoshere. No detailed models exist for the temporal evolution of such mixing and it may well be episodic or fluctuate on relatively short time scales.

G104−27 remains unique among DA white dwarfs in the 25,000–30,000 K temperature range in its failure to be detected at soft X-ray wavelengths (see Fig. 7) which implies that it has additional soft X-ray opacity. New, more sensitive observations of this star from *ROSAT* may lead to a better understanding of the photosphere of G104−27. At this point we can offer no further insight into the issue of trace He in G104−27. It would be prudent, however, to continue to monitor G104−27 at high signal to noise for the possible reappearance of He.

The authors wish to thank Stéphane Vennes for this useful suggestions and to acknowledge the assistance of the Astronomical Data Center with the *IUE* archival data, CfA with the *Einstein* database, and ESTEC for the *EXOSAT* archives and data base. This work was supported by the NASA graduate student researcher program, NASA grant NAG5-434, in the UK by a SERC Advanced Fellowship (MAB) and an SERC Research Studentship (RWT) and in Canada by an NSERC and the Fund FCAR (Quebec).

Note added in proof: after this paper was completed we became aware of the results of Vennes & Fontaine (1992), who reach similar conclusions to ours concerning the effective temperatures of VR 16, GD 125, and GD 222 from an analysis of the *IUE* short-wavelength (SWP) energy distribution.

REFERENCES

Achilleos, N., Wickramasinghe, D. T., Liebert, J., Saffer, R. A., & Grauer, A. D. 1992, ApJ, in press
Barstow, M. A. 1989, in IAU Colloq. 114, White Dwarfs, ed. G. Wegner (Berlin: Springer), 156
———. 1990, MNRAS, 243, 182
Barstow, M. A., Schmitt, J. H. M. M., Clemens, J. C., Pye, J. P., Denby, M., Harris, A. W., & Pankiewicz, G. S. 1991, MNRAS, in press
Barstow, M. A., & Tweedy, R. W. 1990, MNRAS, 242, 484
Bohlin, R. C., & Grillmair, C. J. 1988, ApJS, 68, 487
Cordova, F. A., Rodriguez-Bell, T., Harnden, F. R., Kartje, J., & Mason, K. O. 1991, in Extreme Ultraviolet Astronomy, ed. R. F. Malina & S. Bowyer (New York: Pergamon), 30
Downes, R. A. 1986, ApJS, 61, 569
Finley, D., Basri, G., & Bowyer, S. 1990, ApJ, 359, 483
Finley, D. S., Malina, R. F., & Bowyer, S. 1987, in IAU Colloq. 95, Proc: 2d Conf. on Faint Blue Stars, ed. A. G. D. Philip, D. S. Hayes, & J. W. Liebert (Schenectady: L. Davis), 689
Fontaine, G., & Wesemael, F. 1987, in IAU Colloq. 95, Proc. 2d Conf. on Faint Blue Stars, ed. A. G. D. Philip, D. S. Haynes, & J. W. Liebert (Schenectady: L. Davis), 319
Giommi, P., et al. 1991, ApJ, 378, 77
Gusienov, O. H., Novruzova, H. I., & Rustamov, Y. S. 1983, Ap&SS, 96, 1
Hamada, T., & Salpeter, E. E. 1961, ApJ, 134, 683
Holberg, J. B., Kidder, K. M., & Wesemael, F. 1990, ApJ, 365, L77
Holberg, J. B., Wesemael, F., & Basile, J. 1986, ApJ, 306, 629
Jordan, S., Koester, D., Wulf-Mathies, C., & Brunner, H. 1987, A&A, 185, 253
Kahn, S. M., Wesemael, F., Liebert, J., Raymond, J. C., Steiner, J. E., & Shipman, H. 1984, ApJ, 278, 255
Kidder, K. M. 1991, Ph.D. thesis, University of Arizona
Kidder, K. M., Holberg, J. B., & Mason, P. A. 1991, AJ, 101, 579
Koester, D. 1989, ApJ, 342, 999
Koester, D., Beuermann, K., Thomas, H. C., Graser, U., Giommi, P., & Tagliaferri, G. 1990, A&A, 239, 260
Margon, B., Bolte, M., & Anderson, S. F. 1987, AJ, 93, 1229
McCook, G. P., & Sion, E. M. 1987, ApJS, 65, 603
Morrison, R., & McCammon, D. 1983, ApJ, 270, 119
Paerels, F. B. S., & Heise, J. 1989, ApJ, 339, 1000
Paresce, F. 1984, AJ, 89, 1022
Petre, R., Shipman, H. L., & Canizares, C. R. 1986, ApJ, 304, 356
Pilachowski, C. A., & Milkey, R. W. 1984, PASP, 96, 821
Schmitt, G. 1987, in IAU Colloq. 95, Proc. 2d Conf. on Faint Blue Stars, ed. A. G. D. Philip, D. S. Hayes, & J. W. Liebert (Schenectady: L. Davis), 377
Stern, R. A., Zolcinski, M., Antiochos, S. K., & Underwood, J. H. 1981, ApJ, 249, 647
Thompson, R. 1988, *IUE* Newsletter, 35, 133
Tüg, H., White, N. M., & Lockwood, G. W. 1977, AJ, 61, 679
Vennes, S., & Fontaine, G. 1992, in preparation
Vennes, S. 1990, ApJ, 361, L65
Vennes, S., Pelletier, C., Fontaine, G., & Wesemael, F. 1988, ApJ, 331, 876
Vennes, S., Shipman, H. L., & Petre, R. 1990, ApJ, 364, 647
Vidal, C. R., Cooper, J., & Smith, E. W. 1973, ApJS, 25, 37
Wesemael, F., Auer, L. H., Van Horn, H. M., & Savedoff, M. P. 1980, ApJS, 43, 159